Bull. Mater. Sci. (2019) 42:108
https://doi.org/10.1007/s12034-019-1808-2

Electrical conductivity and pH modelling of magnesium oxide–ethylene glycol nanofluids

MEHDI MEHRABI, MOHSEN SHARIFPUR* and **JOSUA P MEYER**
Department of Mechanical and Aeronautical Engineering, University of Pretoria, Pretoria 0002, South Africa
*Author for correspondence (mohsen.sharifpur@up.ac.za)

MS received 23 September 2018; accepted 20 November 2018; published online 4 April 2019

Abstract. Nanofluids as new composite fluids have found their place as one of the attractive research areas. In recent years, research has increased on using nanofluids as alternative heat transfer fluids to improve the efficiency of thermal systems without increasing their size. Therefore, the examination and approval of different novel modelling techniques on nanofluid properties have made progress in this area. Stability of the nanofluids is still an important concern. Research studies on nanofluids have indicated that electrical conductivity and pH are two important properties that have key roles in the stability of the nanofluid. In the present work, three different sizes of magnesium oxide (MgO) nanoparticles of 20, 40 and 100 nm at different volume fractions up to 3% of the base fluid of ethylene glycol (EG) were studied for pH and electrical conductivity modelling. The temperature of the nanofluids was between 20 and 70°C for modelling. A genetic algorithm polynomial neural network hybrid system and an adaptive neuro-fuzzy inference system approach have been utilized to predict the pH and the electrical conductivity of MgO–EG nanofluids based on an experimental data set.

Keywords. Nanofluids; pH; electrical conductivity; GA-PNN; ANFIS; MgO; ethylene glycol.

1. Introduction

Industrial techniques and technological advancement are continually being tailored towards sustainable development. This is being witnessed in modern manufacturing techniques and devices such as microelectronics, transportation, MEMS and NEMS. The associated thermal management challenges with these new/emerging techniques and devices are very crucial and need urgent attention. In recent decades, nanofluids have been proposed for use as alternative heat transfer fluids in these devices because the conventional heat transfer fluids such as water, engine oil, ethylene glycol etc., have characteristically poor thermal properties. The use of extended surfaces is also often ruled out mainly because they increase the size of equipment. However, there are still challenges with the use of this newly formulated heat transfer fluids (nanofluids). Some of the challenges are the problem of stability, inconsistent enhancement in thermal conductivity, electrical conductivity and excessive increment of effective viscosity.

Thermal conductivity and viscosity of nanofluids have received good attention theoretically and experimentally in order to understand the underlying causes of the inconsistent enhancements [1–6]. Hong *et al* [7] showed that agglomeration formation is one of the underlying factors that affect the enhancement value of nanofluids. They sonicated Fe–EG nanofluids for 30 min (optimal sonication time) and measured the cluster size and thermal conductivity with time after ultrasonication was stopped. One hour after ultrasonication was stopped, their results signified that cluster size increased and the thermal conductivity enhancement reduced from 14.2 to 8.5%. Xuan *et al* [8] and Prasher *et al* [9] also showed that aggregation has a pronounced effect on the behaviour of the thermal conductivity of nanofluids. On the contrary, Putnam *et al* [10] established that well homogenized and stably prepared nanofluids do not display any anomalous enhancement of thermal conductivity.

The theoretical model on a property (thermal conductivity) of a solid–liquid mixture was first established by Maxwell in 1873 [11], followed by Einstein for viscosity in 1906 [1]. Models have been applied to experimental data obtained from different nanofluids with an agreement for low volume concentrations [12,13]. Researchers have shown the lack of a hybrid model for the prediction of nanofluid properties [11,13,14] which are essential to make nanofluids applicable in industries and engineering systems. The mismatches between the experimental data and models are often related to the instability of the nanofluids. Surface active agents (surfactants) or electrostatic charge induction have been proposed to ensure stable nanofluids, a situation where the van der Waals force is lower than the force of repulsion between the particles. In the case of the use of a surfactant which is a kind of chemical method, there is no standard way for adding surfactant to the nanofluid, which gives the possibility of different combinations in the formulation of nanofluids if too much surfactant added to the nanofluid. Electrostatic charging is often reported as an option of making a nanofluid stable too [15].

The stability of nanofluids has been elaborately studied in the open literature using stability markers such as visual

observation (as the starting point), zeta potential measurement, UV-light transmittance analysis, and absorbance, turbidity and sedimentation rate [16]. A detailed explanation on the stability analysis can be found in Adio *et al* [16]. The pH of nanofluids is one of the important parameters to achieve nanoparticle stability in a suspension [17]. Most of the modelling of the properties of nanofluids in the literature is limited to thermal conductivity and viscosity of nanofluids [16,18–27], and there is a lack of modelling for other properties such as pH and electrical conductivities. An adaptive neuro-fuzzy inference system (ANFIS) and genetic algorithm polynomial neural networks (GA-PNN) are two novel approaches that use the advantages of neural network, fuzzy logic and genetic algorithm (GA) methods for modelling the effective pH and the electrical conductivity of magnesium oxide–ethylene glycol (MgO–EG) nanofluids. This was carried out to show the high capability of these two approaches to predict nanofluid electrical conductivity and pH based on an input–output experimental data set as a function of nanoparticle volume concentration, temperature and nanoparticle size.

2. Experimental data used for the training and the testing procedure

Adio *et al* [16] experimentally measured the electrical conductivity and pH of MgO–EG nanofluids in temperatures ranging from 20 to 70°C and the volume concentrations of 0.1–2%. MgO nanoparticles with an average particle size of 20, 40 and 100 nm were used in their study. Transmission electron microscopy (TEM) was used to study the MgO nanoparticles' morphology. The TEM images for the three different nanoparticle sizes corresponded to the manufacturer's estimations. The X-ray diffraction pattern was also obtained using an XPERT-PRO X-Ray Diffractometer, and the resulting patterns matched the Periclase structure (MgO) from the Joint Committee on Powder Diffraction Standards (JCPDS) database. A two-step nanofluid preparation method followed by ultrasonication was used to prepare the MgO–EG nanofluid samples.

pH measurement was carried out using a Jenway 3510 pH meter with -2 to 19.999 pH measurement range and 0.3% measurement accuracy. The meter was calibrated using the inbuilt two-point calibration at 25°C, and the buffer solutions corresponding to these points are 7 and 10 respectively. A CON700 electrical conductivity meter manufactured by EUTECH Instrument was used for electrical conductivity measurements. The electrical conductivity meter was calibrated with a 1413 μS cm^{-1} standard calibration fluid supplied by the manufacturer at 25°C. The temperature of the samples was maintained with the aid of a programmable thermal bath connected to a water jacket. Both meters are equipped with a slope monitor which gives a signal when the measurement does not vary in the range 0.005 and 0.01 for pH and the electrical conductivity meter, respectively.

Adio *et al* [16] measured the electrical conductivity of the base fluid, without the presence of MgO nanoparticles for temperatures ranging from 20 to 70°C. The result indicated that adding MgO nanoparticles to the base fluid steadily increases the electrical conductivity. The electrical conductivity also showed a significant dependency on the temperature, and on increasing the temperature, the electrical conductivity increased too. They also investigated the effect of volume concentration on the electrical conductivity of nanofluids, and they reported that electrical conductivity increases with the increase in the volume fraction.

Adio *et al* [16] also showed that pH of MgO–EG nanofluids with different volume concentrations and particle sizes follows a similar pattern with respect to increase in temperature and further ultrasonication does not affect this trend. They also showed that the temperature variation does not affect the value of pH of the base fluid.

3. Proposed models for the electrical conductivity and pH of MgO–EG nanofluids

3.1 *Proposed models by using ANFIS*

In this paper, the ANFIS approach has been implemented to model the electrical conductivity and pH of MgO/EG nanofluids concerning input parameters of temperature, volume concentration and nanoparticle size. In this study, T (temperature), ϕ (volume concentration) and d_{p} (nanoparticle size) are inputs and the electrical conductivity and pH of MgO/EG nanofluids are the outputs of the system. Generalized bell-shaped membership functions are used for the distribution of input variables. The three inputs (T, ϕ, d_{p}) of the fuzzy inference system are classified into two fuzzy sets each (tables 1 and 2).

Table 1. Premise parameters of the generalized bell-shaped membership function for modelling of the electrical conductivity of MgO/EG nanofluids.

	a_i	b_i	c_i
Temperature (T) (°C)			
MF1	24.99	1.543	20.1
MF2	25.06	0.316	70.12
Volume concentration (ϕ) (%)			
MF1	2.002	1.825	0.4353
MF2	1.896	1.95	2.69
Nanoparticle size (d_p) (nm)			
MF1	40	2.001	20
MF2	40	2.051	100

c_i determines the centre of the corresponding membership function; a_i is the half width and b_i (together with a_i) controls the slopes at the crossover points.

Table 2. Premise parameters of the generalized bell-shaped membership function for modelling of the pH of MgO/EG nanofluids.

	a_i	b_i	c_i
Temperature (T) ($^\circ C$)			
MF1	26.15	1.765	21.13
MF2	23.04	4.572	71.65
Volume concentration (ϕ) (%)			
MF1	1.068	3.413	0.6178
MF2	0.9889	3.022	0.9571
Nanoparticle size (d_p) (nm)			
MF1	39.99	2.072	20
MF2	40	2.013	100

c_i determines the centre of the corresponding membership function; a_i is the half-width and b_i (together with a_i) controls the slopes at the crossover points.

Table 3. Consequent parameters of the proposed ANFIS model for modelling of the electrical conductivity of MgO/EG nanofluids.

Rule no.	p_i	q_i	r_i	c_i
1	0.009484	23.34	1.093	0.05487
2	−0.03289	1.684	−0.02438	0.002173
3	0.3196	22.88	−4.208	−0.2117
4	0.3602	0.8126	0.3006	−0.00632
5	0.2117	34.58	1.015	0.05134
6	0.1856	6.24	−0.1924	0.000341
7	−0.2263	30.76	−4.737	−0.2387
8	0.2673	−3.355	0.5022	−0.0055

Table 4. Consequent parameters of the proposed ANFIS model for modelling of the pH of MgO/EG nanofluids.

Rule no.	p_i	q_i	r_i	c_i
1	−0.02644	0.5997	0.559	0.0279
2	−0.0139	2.707	0.05734	0.001863
3	−0.02617	0.3001	0.5435	0.02705
4	−0.02865	−0.779	0.09148	0.002164
5	−0.01595	0.2321	0.5119	0.02555
6	0.01899	1.557	0.04809	0.001662
7	−0.02823	0.046	0.5884	0.0293
8	−0.03712	−0.3692	0.09157	0.002269

A typical fuzzy rule for our proposed models is as follows:

$$\text{Output (pH or Electrical conductivity)} = p_i \cdot T_i + q_i \cdot \phi_i + r_i \cdot d_{\mathrm{p}_i} + c_i$$

Here p_i, q_i and r_i are referred to as consequent parameters. In tables 3 and 4, these parameters are given for the proposed models. Both of our proposed models have eight fuzzy rules. During training of the ANFIS system for modelling the electrical conductivity and pH of MgO/EG nanofluids, 77 sets of experimental data were used to conduct 1500 cycles of learning and 33 sets of experimental data were reserved for benchmarking. In table 5, statistical criteria that have been used for benchmarking of the proposed models are given. More information on the structure of the ANFIS network is given in Mehrabi *et al* [28] and Rezazadeh *et al* [29].

Table 5. Statistical criteria used for the analysis of the results.

Statistical criterion	Equation
Mean absolute error	$\mathrm{MAE} = \frac{1}{n}\sum_{i=1}^{n}\left\lvert X_{\mathrm{p}} - X_{\mathrm{a}}\right\rvert$
Mean relative error	$\mathrm{MRE}\ (\%) = \frac{100}{n}\sum_{i=1}^{n}\left(\frac{\lvert X_{\mathrm{p}} - X_{\mathrm{a}}\rvert}{X_{\mathrm{a}}}\right)$
Root mean square error	$\mathrm{RMSE} = \sqrt{\frac{1}{n}\sum_{i=1}^{n}\left(X_{\mathrm{p}} - X_{\mathrm{a}}\right)^2}$

X_{p} is the predicted value and X_{a} is the actual (experimental) data.

3.2 *Proposed models by using GA-PNN*

Figure 1 shows the structure of the GA-PNN hybrid system that was used for modelling of the pH and the electrical conductivity of MgO–EG nanofluids. In this hybrid system, GA was applied to determine the group method of data handling (GMDH) polynomial neural network characteristics, such as network weights, bias coefficients and hidden layers in the form of chromosomes through the minimization of the training error. On the other hand, the GMDH was utilized for the learning process of the polynomial neural network. Detailed information about this hybrid system and how different parts are related to each other has been given in Mehrabi *et al* [30,31].

The architectures of GA-PNN models for predicting the pH and the electrical conductivity of MgO/EG nanofluids are shown in figure 2a and b which correspond to the genome representation of *1123122333331312* for the proposed model for the electrical conductivity and *1123222311112312* for the proposed model for the pH in which *1*, *2* and *3* stand for temperature T (°C), volume concentration ϕ and nanoparticle size d_{p} (nm), respectively. The equivalent polynomial models for the electrical conductivity and pH based on network architecture are presented in Appendixes I and II.

3.3 *Results of the proposed models*

Figure 3 shows the comparison of the experimental data and the proposed GA-PNN and ANFIS models for the electrical conductivity of MgO/EG nanofluids with a particle size of 20 nm, volume concentration of 1% in the temperature range of 20–70°C. The ANFIS model predicts the experimental data well (MAE = 1.854, MRE = 14.88% and RMSE = 1.863). The proposed GA-PNN model is also well-matched with the experimental data (MAE = 1.066, MRE = 7.87% and RMSE = 1.249) for lower temperatures and

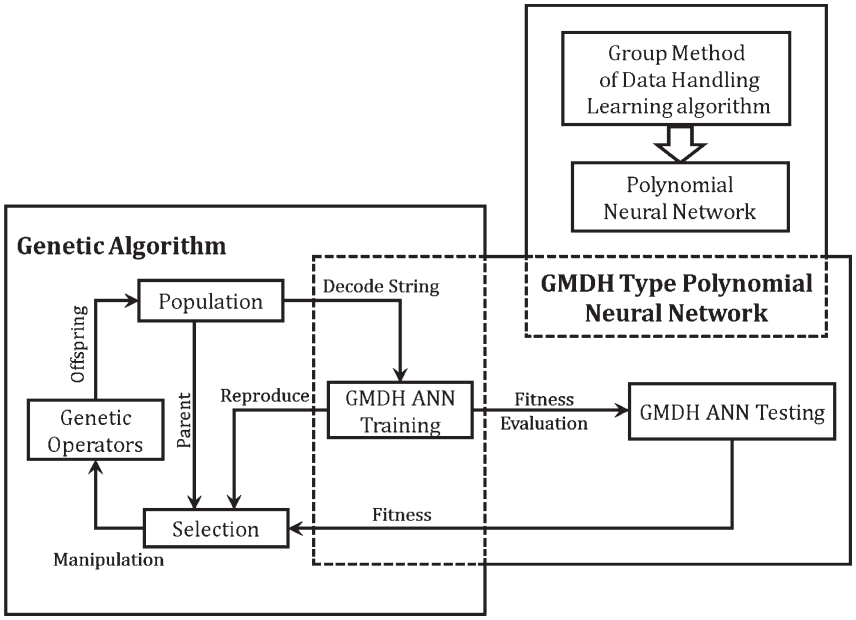

Figure 1. Combination of GA and the GMDH-type polynomial neural network approaches in a hybrid system.

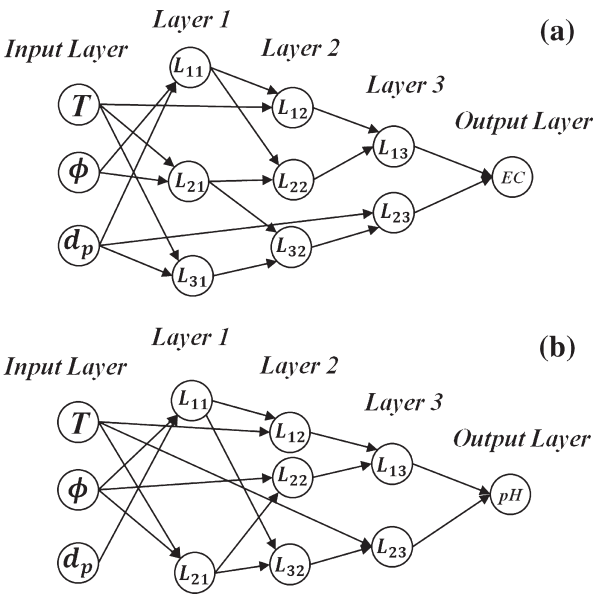

Figure 2. Structure of the GA-PNN hybrid system for (**a**) the electrical conductivity and (**b**) the pH of MgO/EG nanofluids modelling.

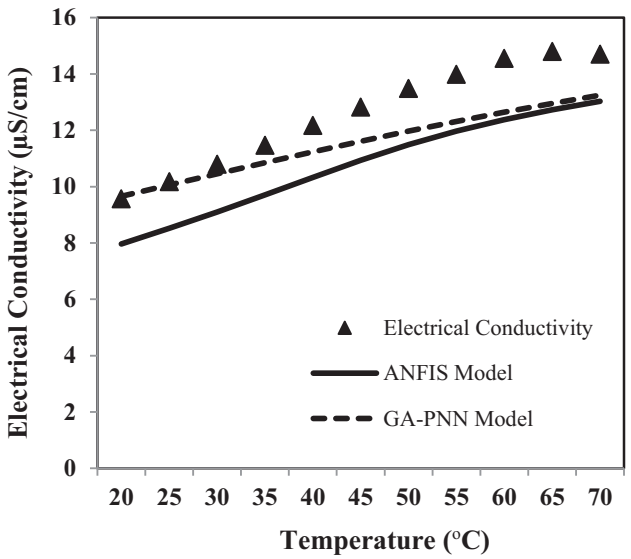

Figure 3. Comparison of the experimental data with the GA-PNN and ANFIS proposed models for the electrical conductivity of MgO/EG nanofluid (MgO/EG nanofluid, with an average particle size of 20 nm at a volume concentration of 1%).

predicts the electrical conductivity better than the ANFIS model.

In figures 4 and 5, the experimental results of the electrical conductivity of the MgO/EG nanofluid with a particle size of 100 nm and two volume concentrations of 0.5 and 2% are compared with the proposed GA-PNN and ANFIS models. Based on the result of figure 4, the ANFIS model (MAE = 1.014, MRE = 10.56% and RMSE = 1.027) is in better agreement with experimental data in comparison with the GA-PNN model (MAE = 1.654, MRE = 17.56% and RMSE = 1.693), and especially in the lower and higher temperature ranges, the ANFIS model shows a better

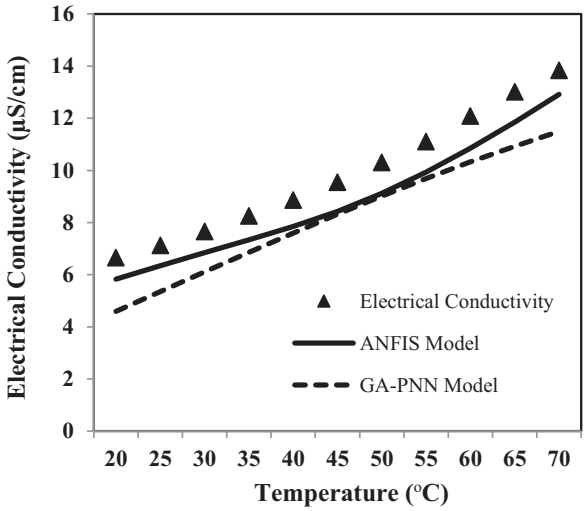

Figure 4. Comparison of the experimental data with the GA-PNN and ANFIS proposed models for the electrical conductivity of MgO/EG nanofluid (with an average particle size of 100 nm at a volume concentration of 0.5%).

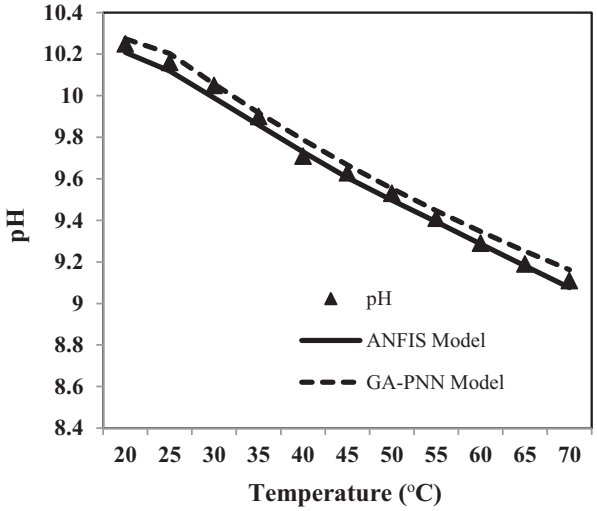

Figure 6. Comparison of the experimental data with the GA-PNN and ANFIS proposed models for the pH of MgO/EG nanofluid (with an average particle size of 20 nm at a volume concentration of 0.5%).

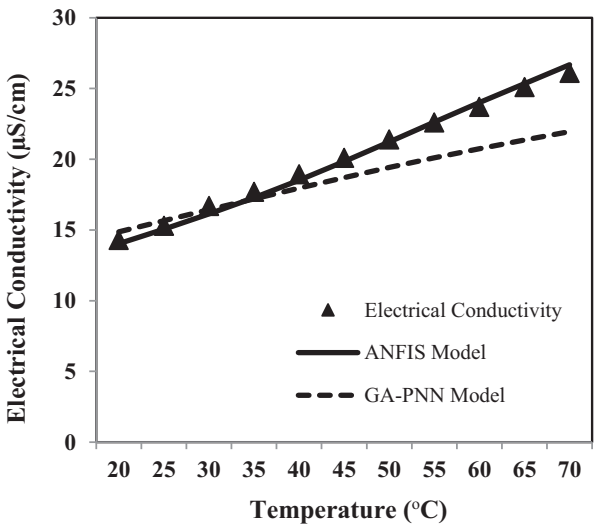

Figure 5. Comparison of the experimental data with the GA-PNN and ANFIS proposed models for the electrical conductivity of MgO/EG nanofluid (with an average particle size of 100 nm at a volume concentration of 2%).

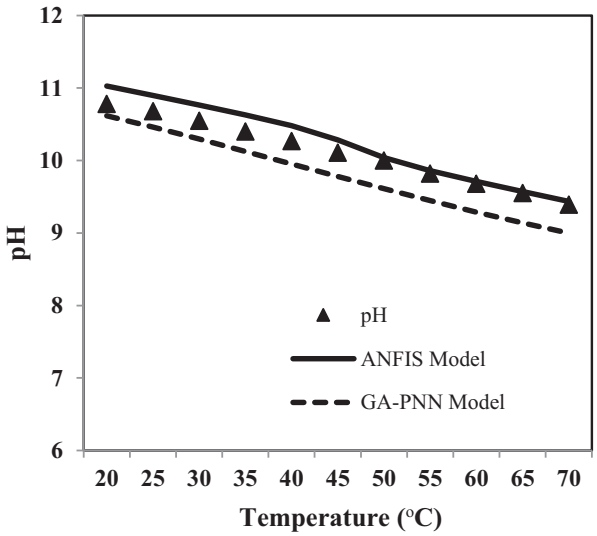

Figure 7. Comparison of the experimental data with the GA-PNN and ANFIS proposed models for the pH of MgO/EG nanofluid (with an average particle size of 20 nm at a volume concentration of 3%).

agreement. Figure 5 shows that the ANFIS model is matched well with experimental data (MAE = 0.318, MRE = 1.64% and RMSE = 0.355) and predicts the electrical conductivity the best. The GA-PNN proposed model is matched well with the experimental data (MAE = 1.762, MRE = 7.85% and RMSE = 2.209) for temperatures lower than 45°C while becoming under-predicted for the experimental data for temperatures higher than 45°C.

Figure 6 shows the experimental data of the pH of MgO/EG nanofluid compared with the GA-PNN model. Also, the ANFIS proposed model for a particle size of 20 nm and volume concentration of 0.5% over a temperature range from 20 to 70°C. Both the proposed models are in very good agreement with the experimental data (MAE = 0.029, MRE = 0.29% and RMSE = 0.033) for the ANFIS model and (MAE = 0.039, MRE = 0.41% and RMSE = 0.044) for the GA-PNN proposed model. The ANFIS model predicts the pH

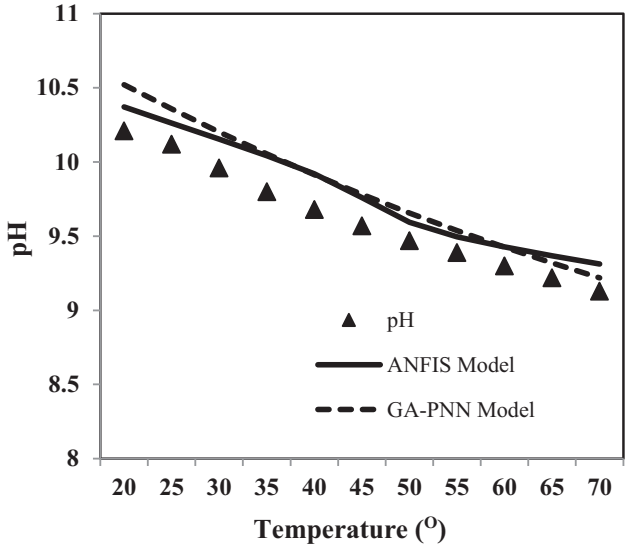

Figure 8. Comparison of the experimental data with the GA-PNN and ANFIS proposed models for the pH of MgO/EG nanofluid (with an average particle size of 100 nm at a volume concentration of 1%).

slightly better than the GA-PNN model, and for the higher temperatures, the ANFIS model output is exactly the same as experimental results.

In figure 7, the experimental results are compared with those of the GA-PNN model and the ANFIS model for the pH of MgO/EG nanofluid with a particle size of 20 nm, and a volume concentration of 3% and temperature ranging from 20 to 70°C. The ANFIS model (MAE = 0.134, MRE = 1.29% and RMSE = 0.162) predicts pH the best when compared with the outputs of the proposed GA-PNN model (MAE = 0.319, MRE = 3.19% and RMSE = 0.329). While the ANFIS model shows a better agreement, the GA-PNN model shows a very good accuracy as well.

Figure 8 shows the outputs of the ANFIS and GA-PNN models for the pH of MgO/EG nanofluid compared with experimental results for a particle size of 100 nm and volume concentration of 1%. For temperature ranging from 30 to 60°C, both the proposed models show the same level of agreement with experimental data while for temperatures lower than 30°C, the ANFIS model (MAE = 0.164, MRE = 1.75% and RMSE = 0.174) predicts the pH better. The GA-PNN model (MAE = 0.145, MRE = 2.0% and RMSE = 0.206) has a better performance for temperatures higher than 60°C.

4. Conclusions

Electrical conductivity and pH behaviour of MgO–EG nanofluids have been investigated with respect to temperature variation, nanoparticles size, sonication time and volume fraction. The experimental results indicated that the electrical conductivity of the nanofluid samples increased significantly with the increase in temperature and volume fraction. However, concerning volume fraction, the electrical conductivity does not follow a simple linear fit which suggests counterion condensation. There is no direct relationship between the MgO nanoparticle size and electrical conductivity; the same trends were obtained from two different ultrasonication times investigated with no significant decrease or increase in electrical conductivity values. Regarding the pH of the MgO–EG nanofluids, it reduces with the increase in temperature and is not significantly affected by the ultrasonication time except at 2% volume fraction. The relative pH plots buttress the fact that size of MgO nanoparticles does not have a direct relationship with the pH values and an increase in volume fraction shows an increase in pH up to the point where the counterion condensation effect was observed to have set in. The significance of the temperature variation in the pH of these nanofluids will be in its effect on the zeta potential. Summarily, pH and electrical conductivity are interrelated, and with the above findings, it is important to note that temperature stable nanofluids could be engineered. This can be achieved by studying the zeta potential of the nanofluids at the pH values as measured in the temperature regime investigated. Then the temperature corresponding to the pH value that gives the best zeta potential or has zeta potential more than ±30 mV (minimum threshold) may represent the temperature at which the nanofluids should be kept for all-time stability.

This study showed the successful application of two GA-PNN and ANFIS approaches for the modelling of the pH and the electrical conductivity of MgO–EG nanofluids as a function of various variables (volume concentration, temperature and nanoparticle size). The results showed that the GA-PNN and the ANFIS methods are accurate and effective.

Appendix I

$$
\begin{aligned}
L_{11} &= a_{1,0} + a_{1,1}\cdot\phi + a_{1,2}\cdot d_{\mathrm{p}} + a_{1,3}\cdot\phi\cdot d_{\mathrm{p}} \\
&\quad + a_{1,4}\cdot\phi^2 + a_{1,5}\cdot d_{\mathrm{p}}^2 \\
L_{21} &= a_{2,0} + a_{2,1}\cdot T + a_{2,2}\cdot\phi + a_{2,3}\cdot d_{\mathrm{p}}\cdot T \\
&\quad + a_{2,4}\cdot T^2 + a_{2,5}\cdot\phi^2 \\
L_{31} &= a_{3,0} + a_{3,1}\cdot T + a_{3,2}\cdot d_{\mathrm{p}} + a_{3,3}\cdot T\cdot d_{\mathrm{p}} \\
&\quad + a_{3,4}\cdot T^2 + a_{3,5}\cdot d_{\mathrm{p}}^2 \\
L_{12} &= a_{4,0} + a_{4,1}\cdot T + a_{4,2}\cdot L_{11} + a_{4,3}\cdot T\cdot L_{11} \\
&\quad + a_{4,4}\cdot T^2 + a_{4,5}\cdot L_{11}^2 \\
L_{22} &= a_{5,0} + a_{5,1}\cdot L_{21} + a_{5,2}\cdot L_{11} + a_{5,3}\cdot L_{21}\cdot L_{11} \\
&\quad + a_{5,4}\cdot L_{21}^2 + a_{5,5}\cdot L_{11}^2 \\
L_{32} &= a_{6,0} + a_{6,1}\cdot L_{31} + a_{6,2}\cdot L_{21} + a_{6,3}\cdot L_{31}\cdot L_{21} \\
&\quad + a_{6,4}\cdot L_{31}^2 + a_{6,5}\cdot L_{21}^2 \\
L_{13} &= a_{7,0} + a_{7,1}\cdot L_{12} + a_{7,2}\cdot L_{22} + a_{7,3}\cdot L_{12}\cdot L_{22} \\
&\quad + a_{7,4}\cdot L_{12}^2 + a_{7,5}\cdot L_{22}^2
\end{aligned}
$$

$$
\begin{aligned}
L_{23} &= a_{8,0} + a_{8,1} \cdot d_{\mathrm{p}} + a_{8,2} \cdot L_{32} + a_{8,3} \cdot d_{\mathrm{p}} \cdot L_{32} \\
&\quad + a_{8,4} \cdot d_{\mathrm{p}}^2 + a_{8,5} \cdot L_{32}^2 \\
\mathrm{EC} &= a_{9,0} + a_{9,1} \cdot L_{13} + a_{9,2} \cdot L_{23} + a_{9,3} \cdot L_{13} \cdot L_{23} \\
&\quad + a_{9,4} \cdot L_{13}^2 + a_{9,5} \cdot L_{23}^2
\end{aligned}
$$

L_{ij} is the i-th output in the j-th layer for the GA-PNN model.

$$
[a_{i,j}] = \begin{bmatrix}
0.027747876 & 3.822604153 & 0.462429558 & -0.374659514 & -0.004205517 & 0.045114086 \\
0.751137821 & 0.145938521 & 5.011703576 & -0.000502634 & -0.103220539 & 0.003901322 \\
0.015971668 & 0.235979845 & 0.266171545 & -0.001501415 & -0.002750727 & 0.001161073 \\
-3.283067536 & 0.095068789 & 0.819407225 & -0.000315974 & -0.000331478 & 0.003277455 \\
1.389849061 & 0.64959239 & 0.116319437 & -0.125388437 & -0.097872314 & 0.235336051 \\
1.193873934 & -0.25706559 & 0.982727589 & 0.012610029 & -0.000454244 & 0.00173388 \\
1.105115316 & 1.489550714 & -0.683855075 & -0.098269034 & -0.027494652 & 0.133113803 \\
0.010619241 & 0.176968505 & 0.67971365 & -0.002261029 & -0.005051182 & 0.008740201 \\
0.028571409 & 1.176834459 & -0.191474172 & 0.057362616 & 0.072612493 & -0.129341963
\end{bmatrix}
$$

Appendix II

$$
\begin{aligned}
L_{11} &= a_{1,0} + a_{1,1} \cdot \phi + a_{1,2} \cdot d_{\mathrm{p}} + a_{1,3} \cdot \phi \cdot d_{\mathrm{p}} \\
&\quad + a_{1,4} \cdot \phi^2 + a_{1,5} \cdot d_{\mathrm{p}}^2 \\
L_{21} &= a_{2,0} + a_{2,1} \cdot T + a_{2,2} \cdot \phi + a_{2,3} \cdot d_{\mathrm{p}} \cdot T \\
&\quad + a_{2,4} \cdot T^2 + a_{2,5} \cdot \phi^2 \\
L_{12} &= a_{3,0} + a_{3,1} \cdot T + a_{3,2} \cdot d_{\mathrm{p}} + a_{3,3} \cdot T \cdot d_{\mathrm{p}} \\
&\quad + a_{3,4} \cdot T^2 + a_{3,5} \cdot d_{\mathrm{p}}^2 \\
L_{22} &= a_{4,0} + a_{4,1} \cdot T + a_{4,2} \cdot L_{11} + a_{4,3} \cdot T \cdot L_{11} \\
&\quad + a_{4,4} \cdot T^2 + a_{4,5} \cdot L_{11}^2 \\
L_{32} &= a_{5,0} + a_{5,1} \cdot L_{21} + a_{5,2} \cdot L_{11} + a_{5,3} \cdot L_{21} \cdot L_{11} \\
&\quad + a_{5,4} \cdot L_{21}^2 + a_{5,5} \cdot L_{11}^2 \\
L_{13} &= a_{6,0} + a_{6,1} \cdot L_{31} + a_{6,2} \cdot L_{21} + a_{6,3} \cdot L_{31} \cdot L_{21} \\
&\quad + a_{6,4} \cdot L_{31}^2 + a_{6,5} \cdot L_{21}^2 \\
L_{23} &= a_{7,0} + a_{7,1} \cdot L_{12} + a_{7,2} \cdot L_{22} + a_{7,3} \cdot L_{12} \cdot L_{22} \\
&\quad + a_{7,4} \cdot L_{12}^2 + a_{7,5} \cdot L_{22}^2 \\
pH &= a_{8,0} + a_{8,1} \cdot d_{\mathrm{p}} + a_{8,2} \cdot L_{32} + a_{8,3} \cdot d_{\mathrm{p}} \cdot L_{32} \\
&\quad + a_{8,4} \cdot d_{\mathrm{p}}^2 + a_{8,5} \cdot L_{32}^2
\end{aligned}
$$

L_{ij} is the i-th output in the j-th layer for the GA-PNN model.

$$
[a_{i,j}] = \begin{bmatrix}
0.033444754 & 0.57742064 & 0.557373458 & -0.096976696 & -0.004692827 & 0.000620553 \\
9.898066327 & -0.023691553 & 1.141784359 & 0.0000969 & -0.210843577 & -0.005661005 \\
-44.23417905 & 0.112053455 & 10.03507958 & 0.0000876 & -0.447629593 & -0.01478803 \\
134.3682947 & 11.80598176 & -28.47847853 & 0.200363275 & 1.615464421 & -1.281415173 \\
-42.30134392 & 12.29220823 & -2.444815909 & -0.732689135 & 0.070198963 & 0.200862777 \\
-1.052141722 & 2.065814262 & -0.846199307 & -0.042050653 & 0.055096649 & -0.024438988 \\
-74.54960615 & 0.253862617 & 15.70866275 & -0.000155682 & -0.718791861 & -0.026399959 \\
0.404458237 & -2.519092266 & 3.422661793 & 2.167188004 & 1.817553076 & -3.979307098
\end{bmatrix}
$$

References

[1] Einstein A 1906 *Ann. Phys.-Berlin* **4** 37
[2] Hatschek E 1913 *Trans. Faraday Soc.* **9** 80
[3] Brinkman H C 1952 *J. Chem. Phys.* **20** 571
[4] Awua J T, Ibrahim J S, Adio S A, Mehrabi M, Sharifpur M and Meyer J P 2018 *Bull. Mater. Sci.* **41** 156
[5] Hong T, Yang H and Choi C J 2005 *J. Appl. Phys.* **97** 064311
[6] Assael M J, Metaxa I N, Kakosimos K and Constantinou D 2006 *Int. J. Thermophys.* **27** 999
[7] Hong K S, Hong T and Yang H 2006 *Appl. Phys. Lett.* **88** 031901
[8] Xuan Y, Li Q and Hu W 2003 *AIChE J.* **49** 1038
[9] Prasher R, Evans W, Meakin P, Fish J, Phelan P and Keblinski P 2006 *Appl. Phys. Lett.* **89** 143119
[10] Putnam S A, Cahill D G, Braun P V, Ge Z and Shimmin R G 2006 *J. Appl. Phys.* **99** 084308
[11] Aybar H S, Sharifpur M, Azizian M R, Mehrabi M and Meyer J P 2015 *Heat Transfer Eng.* **36** 1085
[12] Sharifpur M, Solomon A B, Ottermann T L and Meyer J P 2018 *Int. Commun. Heat Mass* **98** 297
[13] Nwosua Paul N, Meyer J P and Sharifpur M 2014 *Comput. Fluids* **101** 241
[14] Sharifpur M, Yousefi S and Meyer J P 2016 *Int. Commun. Heat Mass* **78** 168
[15] Adio S A, Sharifpur M and Meyer J P 2015 *Heat Transfer Eng.* **36** 1241
[16] Adio S A, Sharifpur M and Meyer J P 2015 *Bull. Mater. Sci.* **38** 1345
[17] Samal S, Satpati B and Chaira D 2010 *J. Alloys Compd.* **504** 389
[18] Sharifpur M, Ntumba T, Meyer J P and Manca O 2017 *Int. Commun. Heat Mass* **85** 12
[19] Adio S A, Mehrabi M, Sharifpur M and Meyer J P 2016 *Int. Commun. Heat Mass* **72** 71
[20] Ntumba T, Sharifpur M and Meyer J P 2016 *Heat Transfer Eng.* **37** 1
[21] Adio S A, Sharifpur M and Meyer J P 2016 *J. Exp. Nanosci.* **11** 630
[22] Sharifpur M, Adio S A and Meyer J P 2015 *Int. Commun. Heat Mass* **68** 208
[23] Chari V D, Sharma D V S G K, Prasad P S R and Murthy S R 2013 *Bull. Mater. Sci.* **36** 517
[24] Hemmat Esfe M, Saedodin S, Bahiraei M, Toghraie D, Mahian O and Wongwises S 2014 *J. Therm. Anal. Calorim.* **118** 287
[25] Hemmat Esfe M, Bahiraei M and Mahian O 2018 *Powder Technol.* **338** 383
[26] Amani M, Amani P, Kasaeian A, Mahian O, Pop I and Wongwises S 2017 *Sci. Rep.-UK* **7** 17369
[27] Amani M, Amani P, Mahian O and Estellé P 2017 *J. Clean Prod.* **166** 350
[28] Mehrabi M, Pesteei S M and Pashaee T 2011 *Int. Commun. Heat Mass* **38** 525
[29] Rezazadeh S, Mehrabi M, Pesteei S M and Mirzaee I 2012 *J. Mech. Sci. Technol.* **26** 3701
[30] Mehrabi M, Rezazadeh S, Sharifpur M and Meyer J P 2012 *ASME 6th International conference on energy sustainability and 10th fuel cell science, Engineering & Technology Conference* (San Diego, CA)
[31] Mehrabi M, Sharifpur M and Meyer J P 2012 *Int. Commun. Heat Mass* **39** 971